frontiers | Frontiers in Earth Science

TYPE Original Research
PUBLISHED 18 April 2023
DOI 10.3389/feart.2023.1158991

OPEN ACCESS

EDITED BY
Hema Achyuthan,
Anna University, India

REVIEWED BY
Ibrahim Ied,
Zagazig University, Egypt
Ikhlas Alhejoj,
The University of Jordan, Jordan
Fadhil Ameen,
University of Sulaymaniyah, Iraq

*CORRESPONDENCE
Sherif Farouk,
geo.sherif@hotmail.com
Tamer Abu-Alam,
tamer.abu-alam@uit.no

SPECIALTY SECTION
This article was submitted to Quaternary Science, Geomorphology and Paleoenvironment, a section of the journal Frontiers in Earth Science

RECEIVED 04 February 2023
ACCEPTED 31 March 2023
PUBLISHED 18 April 2023

CITATION
Farouk S, Jain S, Ahmad F, Abu-Alam T, Al-Kahtany K, El Agroudy IS, Bazeen YS and Shaker F (2023), Multiproxy analyses of paleoenvironmental and paleoceanographic changes during the Danian-Selandian in East Central Sinai: An integrated stable isotope and planktic foraminiferal data.
Front. Earth Sci. 11:1158991.
doi: 10.3389/feart.2023.1158991

Multiproxy analyses of paleoenvironmental and paleoceanographic changes during the Danian-Selandian in East Central Sinai: An integrated stable isotope and planktic foraminiferal data

Sherif Farouk[1]*, Sreepat Jain[2], Fayez Ahmad[3], Tamer Abu-Alam[4,5]*, Khaled Al-Kahtany[6], Ibrahim S. El Agroudy[1], Youssef S. Bazeen[7] and Fatma Shaker[8]

[1]Exploration Department, Egyptian Petroleum Research Institute, Nasr City, Egypt, [2]Department of Geology, School of Applied Natural Science, Adama Science and Technology University, Adama, Ethiopia, [3]Department of Earth and Environmental Sciences, Prince El-Hassan Bin Talal Faculty for Natural Resources and Environment, The Hashemite University, Zarqa, Jordan, [4]The Faculty of Biosciences, Fisheries and Economics, UiT the Arctic University of Norway, Tromsø, Norway, [5]OSEAN—Outermost Regions Sustainable Ecosystem for Entrepreneurship and Innovation, University of Madeira, Colégio dos Jesuítas, Funchal, Portugal, [6]Geology and Geophysics Department, College of Science, King Saud University, Riyadh, Saudi Arabia, [7]Geology Department, Faculty of Science, Al-Azhar University, Cairo, Egypt, [8]Geology Department, Faculty of Science, Benha University, Benha, Egypt

Forty-three planktic foraminifera samples from the Themed section (East Central Sinai; Egypt) spanning the Zone *Parvularugoglobigerina eugubina* (Pα) to the Subzone *Acarinina subsphaerica* (P4b) have been studied. Data from $\delta^{13}C$, $\delta^{18}O$, and planktic foraminifera-based species diversity, depth habitat, preference for warm and cool surface waters, and nutrients (oligotrophic, mesotrophic, and eutrophic conditions) are used to infer paleoenvironmental changes throughout the Danian–Selandian duration. Based on quantitative multivariate analyses (hierarchical cluster and principal component), three distinct intervals were recognized, Interval 1 (Pα–P1b), Interval 2 (P1c–P3a), and Interval 3 (P3a–P4b). Interval 2 is further subdivided into three subintervals, 2a (part P1c), 2b (part P1c), and 2c (P2–P3a). Two $\delta^{13}C$ events are identified, Dan-C2 and Latest Danian Event (LDE) and elaborated concerning paleoenvironmental changes. During the earliest Danian planktic foraminiferal Pα Zone, moderately shallow and eutrophic conditions prevailed with cool surface waters and a shallow thermocline. Comparable conditions were still prevailing during P1a–P1b, but with slightly deeper and mesotrophic conditions and a somewhat deeper thermocline and reduced stratification. P1b–P1c exhibits a major shift from *Eoglobigerina* to *Subbotina–Parasubbotina* with cooler surface waters and moderate mesotrophic conditions. For Subzone P1c (upper part), slightly mesotrophic conditions were inferred, whereas for P2–P3a (lower part), surface water warming and thermocline shallowing events have inferred with increased oligotrophic conditions. The Latest Danian Event (mid-P3a) is marked by a dramatic negative $\delta^{13}C$ excursion, warm waters, increased mesotrophic conditions, and enhanced stratification. The

dominance of *Morozovella*, *Acarinina*, and *Igorina* specify warm and oligotrophic conditions for subzones P3b–P4b.

KEYWORDS

Danian-Selandian, planktic foraminifera, paleoenvironmental, Sinai, Egypt

1 Introduction

There are numerous studies dealing with changes across the Danian/Selandian boundary (D/S) from Egypt (Western and Eastern Desert and Nile Basin) vis-à-vis biostratigraphy and paleoenvironmental changes involving benthic and planktic foraminifera and calcareous nannofossils (see Berggren and Ouda, 2003; Speijer, 2003; Guasti, 2005; Guasti et al., 2005; Guasti and Speijer, 2008; Bornemann et al., 2009; Obaidalla et al., 2009; Youssef, 2009; Sprong et al., 2011; Sprong et al., 2012; Farouk and El-Sorogy, 2015; Hewaidy et al., 2019; Bazeen et al., 2023). In these studies, the emphasis was mainly on the biostratigraphic component (Obaidalla et al., 2009; Farouk and El-Sorogy, 2015; Hewaidy et al., 2017; Bazeen et al., 2023), understanding faunal changes during the D/S boundary event (Guasti, 2005; Guasti et al., 2005; Hewaidy et al., 2019) or with respect to transient bioevents such as the Latest Danian Event (LDE) (Speijer, 2003).

The planktic foraminifera is important not only from the biostratigraphic aspects but also in revealing surface water paleoenvironmental conditions, including water temperature and trophic levels (Boersma and Premoli Silva, 1983; Lu and Keller, 1996; Berggren and Norris, 1997; Pearson et al., 2001). The quantitative paleoenvironmental data on the Danian–Selandian planktic foraminifera from Sinai (Egypt) are limited. Here we present a multiproxy study involving planktic foraminifera coupled with carbon ($\delta^{13}C$) and oxygen ($\delta^{18}O$) isotope data from 43 samples from the Themed section (El Themed village in East Central Sinai) spanning the Danian–Selandian interval. The used proxies include changes in (a) planktic foraminifera species and genera composition, (b) species diversity (the number of species and Fisher's α), and species dominance, (c) changes in the categorization of planktic foraminifera species based on their depth of habitat, preference for warm and cool surface waters, and nutrients (oligotrophic, mesotrophic and eutrophic conditions).

2 Geologic setting

Sinai was situated on the wide northern shelf border of the Afro-Arabian plate that occupies the southern margin of the Tethys Ocean during the Maastrichtian-Paleocene time (Figures 1A,B). The rifts that presently bound the Sinai microplate (Gulf of Suez and Gulf of Aqaba) were still closed. A major transgression of the Tethys Sea occurred during the Paleocene, and large parts of Egypt were flooded, which led to the deposition of a deeper, condensed, and hemipelagic facies, especially during the Paleocene (Farouk, 2016). The shoreline of this transgression probably reached the Gabal Abyad, northern Sudan, where the Paleocene marine sediments similar to the Arabian facies of the Paleocene in southern Egypt have been noted (Barazi and Kuss, 1987). The main units controlling sedimentation in Egypt during the Late Cretaceous and Early Paleogene are the Arabian-Nubian massif and the tectonically "Stable Shelf" in south and central Egypt, and the "Unstable Shelf" in the north (Said, 1962). The Paleocene succession in Sinai comprises the following formations, Dakhla, Tarawan Formation, and the lower part of Esna. The Dakhla Formation is represented by hemipelagic calcareous mudstones and marls, with much-reduced thickness than noted in other parts of Egypt (Figure 2). In Sinai, the Dakhla Formation occurs between two carbonate intervals overlying the Campanian–Maastrichtian Sudr Formation and underlying the Tarawan Formation (Figure 2). Due to distinct lateral facies changes, the Dakhla Formation is restricted to Danian–Selandian time interval in northern Egypt (Sinai). In contrast, in central and southern parts of Egypt, the argillaceous facies of the Dakhla Formation extends in age from the Maastrichtian to Selandian (Farouk, 2016; Bazeen et al., 2023).

3 Materials and methods

The studied section occurs 5 km west away from El Themed village in East Central Sinai (29°46′39.11″N and 34°15′52.00″E; Figure 1A). In the present study, *Morozovella*, *Acarinina,* and *Igorina* are considered as warm water genera, whereas cool water taxa include *Parasubbotina* and *Subbotina*; the keeled genera include *Morozovella* and *Igorina* (Speijer, 2003; Guasti, 2005; Bornemann et al., 2009; Bornemann et al., 2021). Additionally, the planktic foraminifera species are also categorized based on their depth habitat, as corroborated by isotopic studies (Table 1 and references therein). These include (a) mix-layer with photosymbionts, (b) mix-layer (superficial waters/shallower pelagic dwellers), and (c) thermocline and sub-thermocline (deeper pelagic dwellers) (see Table 1). Both mix-layer and mix-layer with photosymbionts inhabit the shallower portions of the water column suggesting oligotrophic conditions for the water column, whereas the thermocline and sub-thermocline forms inhabit the lower part of the water column and suggest a pelagic ecosystem with the development of a well-stratified water column and mesotrophic conditions (Krahl et al., 2017; see also Table and references therein). To measure the preservation degree of the planktic foraminiferal assemblages, the following criteria were adopted: E = excellent (sample includes "glassy" shells with no evidence of recrystallization or secondary mineral infilling or overgrowth); G = good ("frosty" shells with minor recrystallization, but no evidence of secondary mineral infilling or overgrowth); M = moderate (opaque shells with minor to significant shell recrystallization, presence of secondary mineral infilling or overgrowth); P = poor (shells strongly recrystallized and infilled or strongly fragmented). Hierarchical cluster analysis (Ward's method) and Principal Component Analysis (PCA)

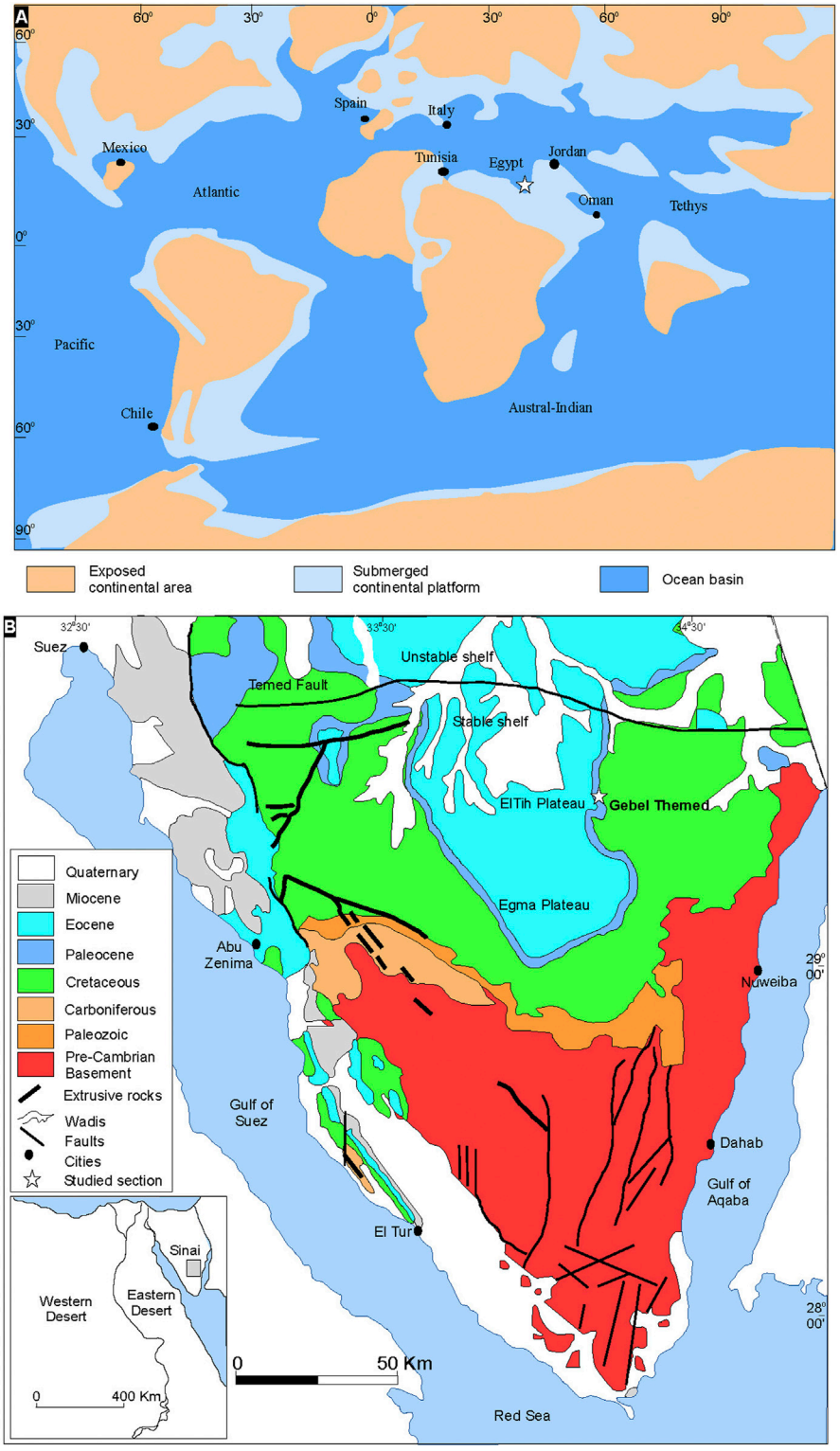

FIGURE 1
(A) Danian paleogeographic position of the study area (modified after Macleod and Keller, 1991). **(B)** Simplified geologic map of Sinai showing the location of the study section (adapted after the Geological Survey of Egypt, 1994).

are used to define intervals. Species diversity is measured by using four components: species richness (the number of species), species dominance (the degree to which one or several species have a significant influence controlling the other species in their ecological community), and the Shannon H (the index accounts for both abundance and evenness of the species present); all analyses were

FIGURE 2
Outcrop of Themed section showing exposures of the Dakhla, Tarawan, Esna and Thebes formations.

done with the software PAST, Paleontological Statistics (Hammer et al., 2001). The values of species evenness and dominance range from 0 to 1; higher values of species evenness suggest an equitable environment, whereas higher values of species dominance denote the dominance of a particular species. Forty-two rock samples were analyzed for $\delta^{13}C$ and $\delta^{18}O$ isotopes at the Environmental Isotope Laboratory, University of Arizona. For more detailed methods, see Salhi et al. (2022).

4 Results

4.1 Biostratigraphy

The studied samples of the Themed section show moderately diverse and abundant planktic foraminiferal assemblages ranging in age from earliest Danian to Selandian, subdivided into five zones, following the biozonal schemes of Berggren et al. (2005) and Wade et al. (2011) (Figure 3).

The distinctive earliest Danian planktic foraminifera *Parvularugoglobigerina eugubina* was recorded in the basal two samples (3 and 4), permitting the identification of Zone Pα (Figure 3). This also indicate the absence of the P0 Zone which may refer to a brief time gap at the Cretaceous/Paleogene boundary. The dominant species of this zone include *Eoglobigerina eobulloides, Eoglobigerina edita, Eoglobigerina simplicissima, Parasubbotina moskvini, Praemurica pseudoinconstans, Pr. taurica, Woodringina claytonensis* and *W. homerstownensis* (Figure 3).

The *E. edita* (P1) Zone is noted between samples 5–30 (Figure 3) and is defined as the partial range of the nominal species between the Highest Occurrence (HO) of *P. eugubina* and the Lowest Occurrence (LO)*Praemurica uncinata* (Figure 3). The P1 Zone is further divided into three subzones, P1a, P1b, and P1c, based on the sequential LO of *Subbotina triloculinoides* and *Globanomalina compressa* (Berggren et al., 2005). The P1a Subzone encompasses samples 5–7 (Figure 3). The foraminiferal species are similar to those of the underlying Pα Zone, except the absence of the nominated taxon. During this subzone, some species have their HO, such as *Eoglobigerina fringe*, *E. simplicissima*, and *Globanomalina archeocompressa* (see Figure 3).

The P1b Subzone is represented by the sequential LOs of *Subbotina triloculinoides* and *G. compressa*, reported from two successive samples, 8 and 9, respectively (Figure 3). The P1c Subzone is bracketed between the sequential LOs of *G. compressa* and *Praemurica uncinata* (samples 9–30; Figure 3). The planktic species of the P1b Subzone are similar to those of the P1a Subzone, except for the LO of *Subbotina triloculinoides* (Figure 3). The P1c Subzone yields several planktic foraminifera bioevents such as the LOs *Praemurica inconstans*, *Pr. trinidadensis*, and *Globanomalina imitate*, and the HOs of *P. moskvini*, *Praemurica taurica*, *W. claytonensis*, *Praemurica pseudoinconstans*, *E. eobulloides*, in chronological order (see Figure 3).

The *Praemurica uncinata* (P2) Zone, defined by the LOs of *Praemurica uncinata* and *Morozovella angulata*, which spans a short time interval (61.4–61 Ma; Wade et al., 2011), is noted between samples 31–33 (Figure 3). This zone exhibits the LOs of *Eoglobigerina spiralis*, *Globanomalina ehrenbergi*, *Subbotina cancellata*, *Subbotina triangularis*, and *Morozovella praeangulata*. The lower boundary of this zone is defined by the HO of *E. edita* and the upper boundary by the HO of *Subbotina trivialis* (Figure 3).

The *M. angulata* (P3) Zone is defined by the LOs of *M. angulata* and *Globanomalina pseudomenardii* (Figure 3). This zone is divided into two subzones, P3a and P3b, based on the LO of *Igorina albeari* (Berggren et al., 2005; Wade et al., 2011). In the present study, the

P3a Subzone (samples 34–37) exhibits the LOs of the *Igorina pusilla*, *M. angulata*, *Morozovella conicotruncata*, *P. variospira*, *Acarinina hansibolli,* and *Acarinina strabocella* (see Figure 3). The P3b Subzone (samples 38–39) and marks a major shift in planktic foraminifer species composition, typified by the demise of pramuricids and eoglobigerinids and the dominance of morozovellids (*M. angulata*, *Morozovella apanthesm*, *Morozovella occlusa*, and *Morozovella velascoensis*) (see Figure 3).

The *G. pseudomenardii* (P4) Zone is marked by the nominate taxon's total range. It includes subzones P4a, P4b, and P4c, whose boundaries are delimited by the HO of *Parasubbotina variospira* and the LO of *Acarinina soldadoensis* (Berggren et al., 2005; Wade et al., 2011). In the present study, only the lower two subzones (P4a and P4b) are identified (see Figure 3). The lower Subzone P4a spans from the LO of *G. pseudomenardii* to the HO of *P. variospira* (samples 40–43). The planktic foraminifer of this subzone is somewhat similar to that of the underlying P3b Subzone except for the LO of *G. pseudomenardii* (see Figure 3). The P4b Subzone is defined as a partial range of *Acarinina subsphaerica* between the HO of *P. variospira* and the LO of *A. soldadoensis* (Figure 3). Subzone P4b straddles the topmost portion of the investigated section, samples 44–45 (Figure 3). Hence, the upper boundary of this subzone is not detected. This subzone is marked by the LOs of *Acarinina nitida*, *Zeauvigerina aegyptiaca,* and *Igorina tadjikistanensis* (see Figure 3).

4.2 Carbon and oxygen isotopes

4.2.1 Carbon isotope

The $\delta^{13}C$ values exhibit fluctuations between 1.96‰ and −0.1‰ (Figure 4). Two $\delta^{13}C$ events are identified in the present study, Dan-C2 event (Dan-C2) and the Latest Danian Event (LDE) (Figure 4). Two more events are suggested *viz.*, Lower Chron 29n event (L. C29n) and the Middle Chron 27r event (M. C27r) (Figure 4). However, higher resolution data is needed to conclusively confirm the presence of the latter two events. Both Dan-C2 and LDE events are elaborated below.

4.2.2 Dan-C2 hyperthermal event

The Dan-C2 hyperthermal event has been well-documented at sites in the Atlantic Ocean and is characterized by double, fairly symmetrical negative excursions in carbon ($\delta^{13}C$) and oxygen ($\delta^{18}O$) isotopes in bulk sediment and is associated with an increase in sediment clay content and a decrease in carbonate content (Kroon and Zachos, 2007; Quillévéré and Norris, 2008; Barnet et al., 2017; Barnet et al., 2019). However, the event might have been restricted to the Atlantic and surrounding areas, including the Tethys Ocean (e.g., Westerhold et al., 2011). A Dan-C2 negative Carbon Isotope Excursion (CIE) was identified at ODP Hole 1049C (NW Atlantic) in bulk sediment (~1.3‰), planktic (~0.7‰), and benthic foraminifera (~1‰), and in bulk sediment in Deep Sea Drilling Project (DSDP) Holes 527 and 528 (SE Atlantic; ~1.5‰ and ~0.8‰ respectively) (Quillévéré and Norris, 2008). In western Tethys (Gubbio section), the Dan-C2 is observed in bulk $\delta^{13}C$ (~0.8‰) (Coccioni et al., 2010). This event is also recorded at the Wadi Hamma section in Egypt (Punekar et al., 2014; Figure 4). In the present study, the Dan-C2 event is characterized by a sudden

TABLE 1 Paleoecological significance of species identified in the present study. 1, Shackleton (1985); 2, D'Hondt et al. (1994); 3, Aze et al. (2011); 4, Berggren and Norris (1997); 5, Lu and Keller (1996); 6, Boersma and Premoli Silva (1983); 7, D'Hondt and Zachos (1993); 8, Olsson et al. (1999); 9, Pearson et al. (2001); 10, Coxall et al. (2000); 11, Huber and Boersma (1994).

Species	Habitat	References
Parvularugoglobigerina alabamensis	Mix-layer	7,8
Parvularugoglobigerina eugubina		7,8
Parvularugoglobigerina longiapertura		7,8
Praemurica inconstans		4,6
Praemurica pseudoinconstans		3
Praemurica taurica		4,7
Praemurica uncinata		1,4
Rectoguembelina cretacea		11
Woodringina claytonensis		8
Woodringina hornerstownensis		7,8
Woodringina irregularis		11
Praemurica nikolasi		11
Acarinina strabocella	Mix-layer with photosymbiosis	3
Igorina albeari		3
Igorina pusilla		3
Igorina tadjikistanensis		4
Morozovella acutispira		4
Morozovella angulate		1,6
Morozovella apanthesma		4,5
Morozovella conicotruncana		4,6
Morozovella praeangulata		1
Morozovella velascoensis		4
Parasubbotina pseudobulloides	Subthermocline	4,7
Chiloguembelina midwayensis	Thermocline	6,7
Chiloguembelina morsei		6,7
Chiloguembelina subtriangularis		6,7
Eoglobigerina edita		3
Eoglobigerina eobulloides		4,7
Eoglobigerina spiralis		3
Globanomalina archeocompressa		3
Globanomalina compressa		8
Globanomalina ehrenbergi		3
Globanomalina imitate		3
Globanomalina planocompressa		8
Globanomalina pseudomenardii		4

(Continued on following page)

TABLE 1 (*Continued*) **Paleoecological significance of species identified in the present study. 1, Shackleton (1985); 2, D'Hondt et al. (1994); 3, Aze et al. (2011); 4, Berggren and Norris (1997); 5, Lu and Keller (1996); 6, Boersma and Premoli Silva (1983); 7, D'Hondt and Zachos (1993); 8, Olsson et al. (1999); 9, Pearson et al. (2001); 10, Coxall et al. (2000); 11, Huber and Boersma (1994).**

Species	Habitat	References
Globoconusa daubjergensis		6
Parasubbotina varianta		8,9
Parasubbotina varioespira		8,9
Subbotina trivialis		10
Subbotina triangularis		2,10
Subbotina velascoensis		4,10
Subbotina triloculinoides		4,10
Zeauvigerina waiparaensis		11

decrease in $\delta^{13}C$ values from 0.47‰ (sample 6) to −0.27‰ (sample 7) (Figure 4).

4.2.3 Latest Danian Event (LDE)

The Carbon Isotope Excursion (CIE) associated with the Late Danian Event (LDE) has not been recorded in Tunisian sections (Sprong et al., 2013). The negative $\delta^{13}C$ excursion observed at the base of the Selandian at the Zumaia section (Schmitz et al., 1998) is not recorded in some sections (Berggren et al., 2000). On the other hand, the LDE is marked in some sections by a double-peak carbon isotope excursion (Monechi et al., 2013). The negative $\delta^{13}C$ excursion at the base of the late Danian and the base of Selandian at the Zumaia section is probably related to sea-level fall that may have shifted the coastline closer to Zumaia (Schmitz et al., 2011).

In the present study, a sudden decrease in $\delta^{13}C$ from 1.19‰ to −0.10‰ (samples 35–37) characterizes the Late Danian Event (LDE) at the Chron C27n/C26r boundary within the uppermost part planktic foraminiferal P3a Subzone (Figure 4). This negative $\delta^{13}C$ shift also coincides with decreasing $\delta^{18}O$ values (Figure 4), reflecting an exceptional perturbation of the carbon cycle and sea level fall (Jarvis et al., 2002), indicating warming of bottom and surface waters of up to 2 C of the deep ocean during the early Paleocene global warming episode (Westerhold et al., 2011).

4.3 Oxygen isotope

The overall negative values of the $\delta^{18}O$ isotope fluctuate between −2.7 and −4.05‰, suggesting they are unstable and very variable (Figure 4). About two-thirds of the readings lie between −2.3 and −3.3. (Figure 4). The studied $\delta^{18}O$ interval (samples 1–14) have higher negative values ranging from −2.31‰ (sample 4) to −4.9‰ (sample 14) (Figure 4). The second interval occurs within the upper part of Subzone P1c and Zone P2, ranging from 2.20 (sample 33) to −3.26‰ (sample 26) (Figure 4). The third interval occurs across the D/S boundary (samples 34–40) ranging from −2.9 (sample 35) to −3.64‰ (sample 34) (Figure 4). The upper interval (samples 41–45; within Zone P4) is characterized by increased values ranging from −2.07‰ (samples 43) to −2.52‰ (sample 44) (Figure 4).

4.4 Preservation and diagenesis

Of the studied 43 samples, only three ample showed poor preservation (samples 30, 36, and 37), whereas one sample showed very poor preservation (sample 43) and one with poor to moderate preservation (sample 44) (see Figure 3). The remaining 38 samples showed moderate to good preservation. The preservation of all samples was good enough to confidently assign species-level identifications (Figure 3).

Diagenesis impacts the rock's primary isotopic signature, which, in turn, influences the reliability of the recognized trends and patterns among the measured values. The oxygen isotope values are more sensitive to diagenetic alteration than carbon isotope values (Allan and Matthews, 1982; Jenkyns et al., 1994). Therefore, cross-plotting the measured $\delta^{13}C$ vs. $\delta^{18}O$ values has been adopted as an adequate strategy to assess the originality of the carbon isotope signature (Jarvis et al., 2011). Higher positive co-variance between $\delta^{13}C$ and $\delta^{18}O$ denotes diagenesis within the marine-meteoric mixing zone (Allan and Matthews, 1982). In this regard, the present $\delta^{13}C$ and $\delta^{18}O$ cross-plots reveal a weak correlation ($R^2 = 0.219$) and a moderate positive correlation coefficient (0.46), suggesting reduced co-variance (20%) between $\delta^{13}C$ and $\delta^{18}O$, signaling less diagenetic influence of the carbon isotopic signature (Figure 5). Whereas the present $\delta^{18}O$ measurements show normal distribution with values ranging from −2.7 to −4.05, the $\delta^{13}C$ measurements are somewhat right skewed, where most values (58.5%) plot between 0.2‰ and 0.6‰ (Figure 5). Furthermore, moderate to good species preservation suggests relatively less diagenetic overprinting and the reliability of the primary signal.

4.5 Planktic foraminiferal distribution

In the present study, 44 planktic foraminiferal species are identified. Among them, 16 species account for 84% of the total planktic foraminiferal population (Figure 3). Of these sixteen species, four dominate and make up 50% of this population; these are *Subbotina triloculinoides* (15.4%), *Parasubbotina pseudobulloides* (14.1%), *Parasubbotina varianta* (13.6%) and *Praemurica inconstans* (7.9%) (Figure 3).

Based on quantitative multivariate analyses (hierarchical cluster and principal component), three intervals of change are identified, Interval 1 to 3; Interval 2 is further subdivided into three subintervals, 2a, 2b, and 2c (Figure 6). These intervals/subintervals are briefly described below.

4.5.1 Interval 1 (samples 3–8; Pα–P1b zones)

Six species dominate this interval, *E. eobulloides* (13.2%), *Praemurica taurica* (12.1%), *P. moskvini* (11.5%), *E. edita* (8.5%), *Praemurica pseudoinconstans* (8.5%) and *E. simplicissima* (8.5%) (Figure 3). In terms of the genus level, three genera dominate,

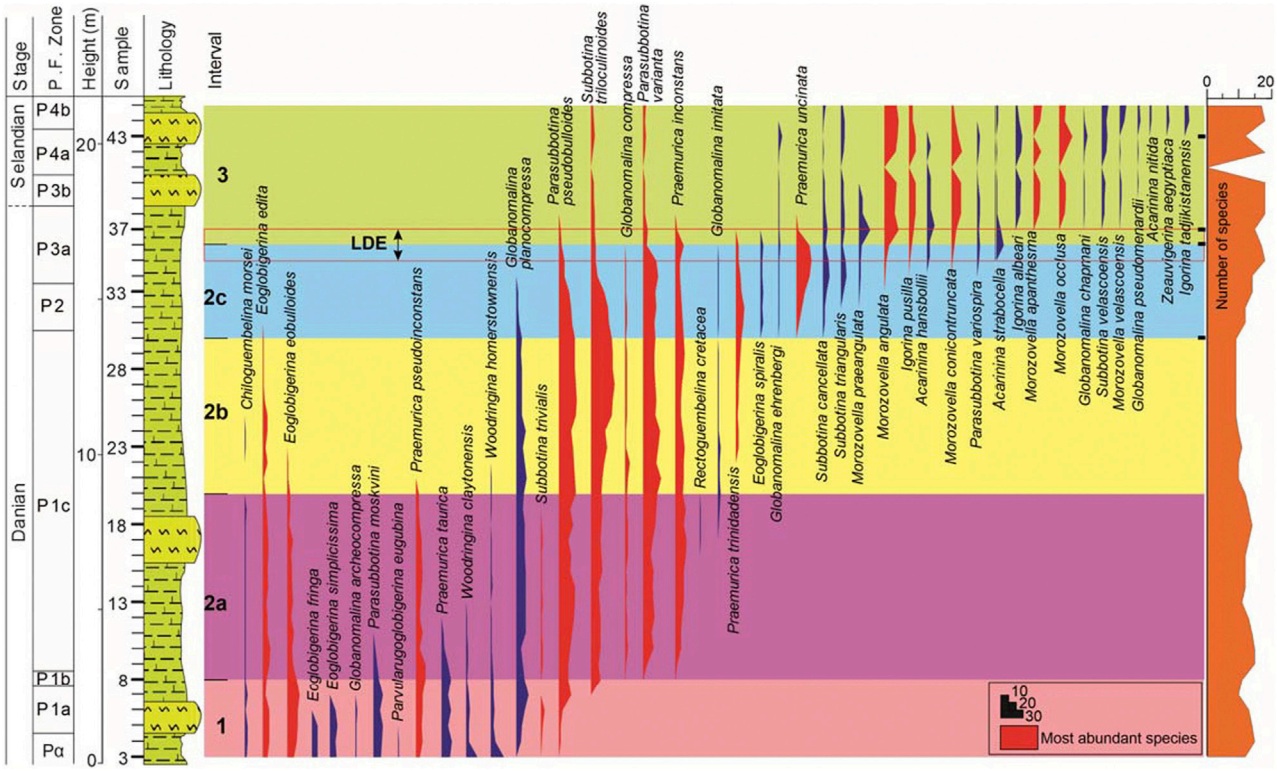

FIGURE 3
Distribution of identified planktic foraminifera species from the Themed section (El Themed village in East Central Sinai, Egypt). The identified zones (1–3) are based on hierarchical clustering and principal component analysis. Of the 44 identified planktic foraminifera species, 16 (in red) make up 84% of the total population. Changes in the number of taxa is also shown on the right (see text for further explanation).

Eoglobigerina (36.1%), *Praemurica* (20.4%), and *Parasubbotina* (14.4%) (Figure 7). This interval is dominated by thermocline dwellers (deeper pelagic dwellers) ranging from 48% to 74% (average, 66%) with lower values of mix-layer dwellers (shallower pelagic dwellers) ranging from 26% to 52% (average, 34%); the thermocline dwellers increase gradually, whereas, the mix-layer dwellers decrease, correspondingly, from 52% to 33% (average, 34%) (see Figure 3). The cool water taxa (*Parasubbotina* and *Subbotina*), from the base to the top, show increasing values ranging from 27% to 46%, with an average of 38.9% (Figure 3). The interval is marked by moderately low diversity values (number of species from 11 to 15, average 12.5; Fisher's α ranging from 2.8 to 4.9, average 3.8) with very low species dominance values, from 0.09 to 0.13 (average 0.11) (see Figure 3). The $\delta^{13}C$ values remain low and range from 0.26% to 0.47% with an average value of 0.36% (Figure 3).

4.5.2 Interval 2 (samples 9–36; P1c–P3a subzones)

The subintervals of Interval 2 are based on changes in the distribution of three dominant species (*P. varianta*, *Subbotina triloculinoides,* and *P. pseudobulloides*) and genera (*Parasubbotina*, *Subbotina,* and *Praemurica*) (see Figures 3, 7). Interval 2 also marks a shift in species composition and generic abundance from *Eoglobigerina* (36.1%; *E. eobulloides*: 13.2%) in Interval 1 to *Subbotina–Parasubbotina* (*S. triloculinoides* and *P. pseudobulloides*, 20.5% each) in Interval 2 (see Figures 3, 7).

4.5.2.1 Subinterval 2a (samples 9–20; part P1c)

In Subinterval 2a, six species make up 77% of the total planktic foraminiferal population, *P. pseudobulloides* (18.4%), *P. varianta* (14.7%), *S. triloculinoides* (13.4%), *Subbotina trivialis* (12.2%), *Praemurica inconstans* (11.5%) and *Praemurica pseudoinconstans* (7.2%) (Figure 3). In terms of genera, *Parasubbotina* (33.5%), *Subbotina* (25.6%), and *Praemurica* (19.5%) make up 79% of the total planktic foraminiferal population (Figure 7). All species show a gradual increase in relative abundances; *P. pseudobulloides* (from 12.4% to 23.9%; average: 18.2%), *P. varianta* (from 5.2% to 20.4%; average: 14.6%), *S. triloculinoides* (from 10.7% to 14.5%; average: 1.34%), *Subbotina trivialis* (from 9.9% to 10.4%; average: 11.7%) and *P. inconstans* (from 2.6% to 10.7%; average: 10.9%); *Pr. pseudoinconstans* shows a declining trend (from 13.7% to 3.8%; average: 7.2%) (Figure 3). The Subinterval 2a is also marked by declining values of number of taxa (base to top: from 15 to 12; averaging 13) and Fisher's α (from 4.9 to 3.6; averaging 4) with a corresponding increase in species dominance (from 0.09 to 0.15; averaging 0.12) (Figures 3, 7). The interval is also dominated by increasing values of the thermocline dwellers (deeper pelagic dwellers), from 68% to 84% with an average value of 78% with correspondingly lower values of mix-layer dwellers (shallower pelagic dwellers), increasing from 32% to 16% with an average value of 22% (Figure 7). The cool water species of *Parasubbotina* and *Subbotina* genera show increasing and highest values, increasing from 64% to 67% with an average

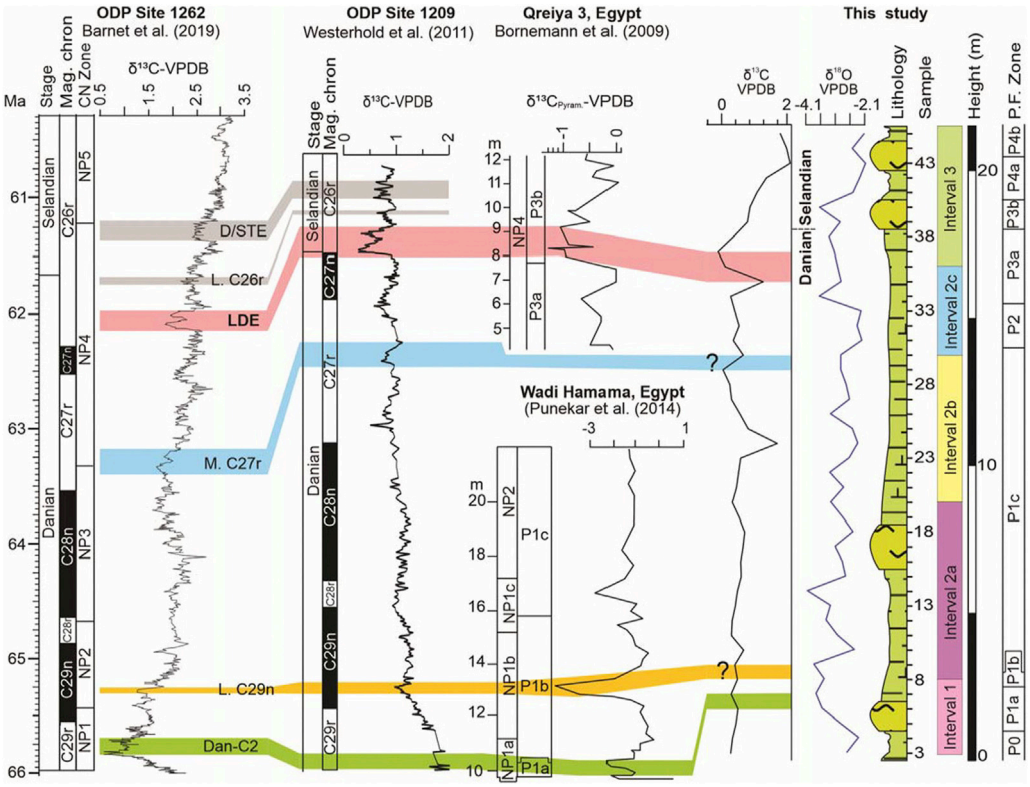

FIGURE 4
Correlation of $\delta^{13}C$ isotope curves of ODP (Ocean Drilling Program) sites 1262 and 1269, Qreiya and Wadi Hamama sections (Egypt) and the Themed section (present study).

value of 59% (Figure 7). The $\delta^{13}C$ values remain low but show increasing values, from 0.38% to 0.31% with an average value of 0.47% (Figure 7).

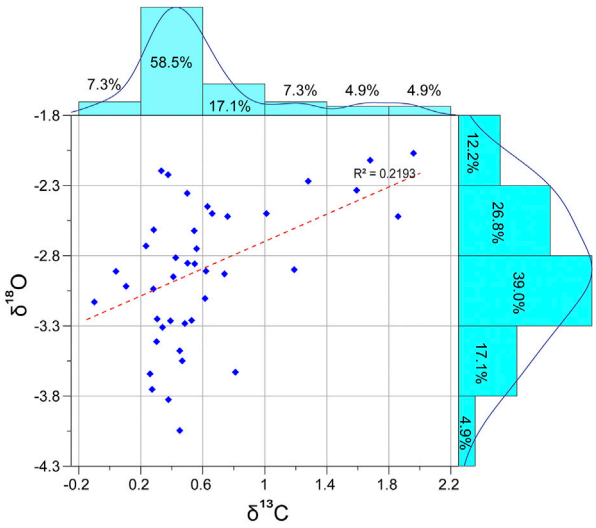

FIGURE 5
Histograms illustrating the distribution of the $\delta^{13}C$ *versus* $\delta^{18}O$ data. The cross-plots show a weak correlation (R^2 = 0.219).

4.5.2.2 Subinterval 2b (samples 21–30; part P1c)

In Subinterval 2b, five species make up 88% of the total planktic foraminiferal population, *Subbotina triloculinoides* (26.9%), *P. pseudobulloides* (22.4%), *P. varianta* (18.5%), *Praemurica inconstans* (11%) and *Subbotina trivialis* (8.9%) (Figure 3). In terms of the genera, *Parasubbotina* (41%), *Subbotina* (36%) and *Praemurica* (16%) make up 93% of the total planktic foraminiferal population (Figure 3). Of the five most abundant species, two species show increasing trends, *S. triloculinoides* (15.1%–27.8%; average 25.1%) and *P. pseudobulloides* (22.4%–22.7%; average 22%), whereas the other three species show declining trends, *P. varianta* (25.4%–17.7%; average 19.4%), and *Pr. inconstans* (12%–1.4%; average 11.1%) and *Subbotina trivialis* (14.4%–8.5%; 9.7average %) (Figure 3). The Subinterval 2b is also dominated by thermocline dwellers with an average value of 85%, but (from the base to the top) shows slight declining values, from 87.3% to 80% (Figure 7). The values for the mix-layer dwellers remains low (averaging 15.1%), although they show an increasing trend, from 12.7% to 20% (Figure 7). The cool water species (of *Parasubbotina* and *Subbotina*) remain high and largely unchanged from the previous subinterval; their values for this subinterval range from 77.3% to 76.7% with an average of 76% (Figure 7). Declining species diversity values (number of taxa from 10 to 9, averaging 9.5, and Fisher's α from 2.8 to 2.4, averaging 2.6) are also noted in this subinterval. However, species dominance (from 0.18 to 0.19; averaging 0.18) only shows negligible change (Figure 7). The $\delta^{13}C$ values remain low

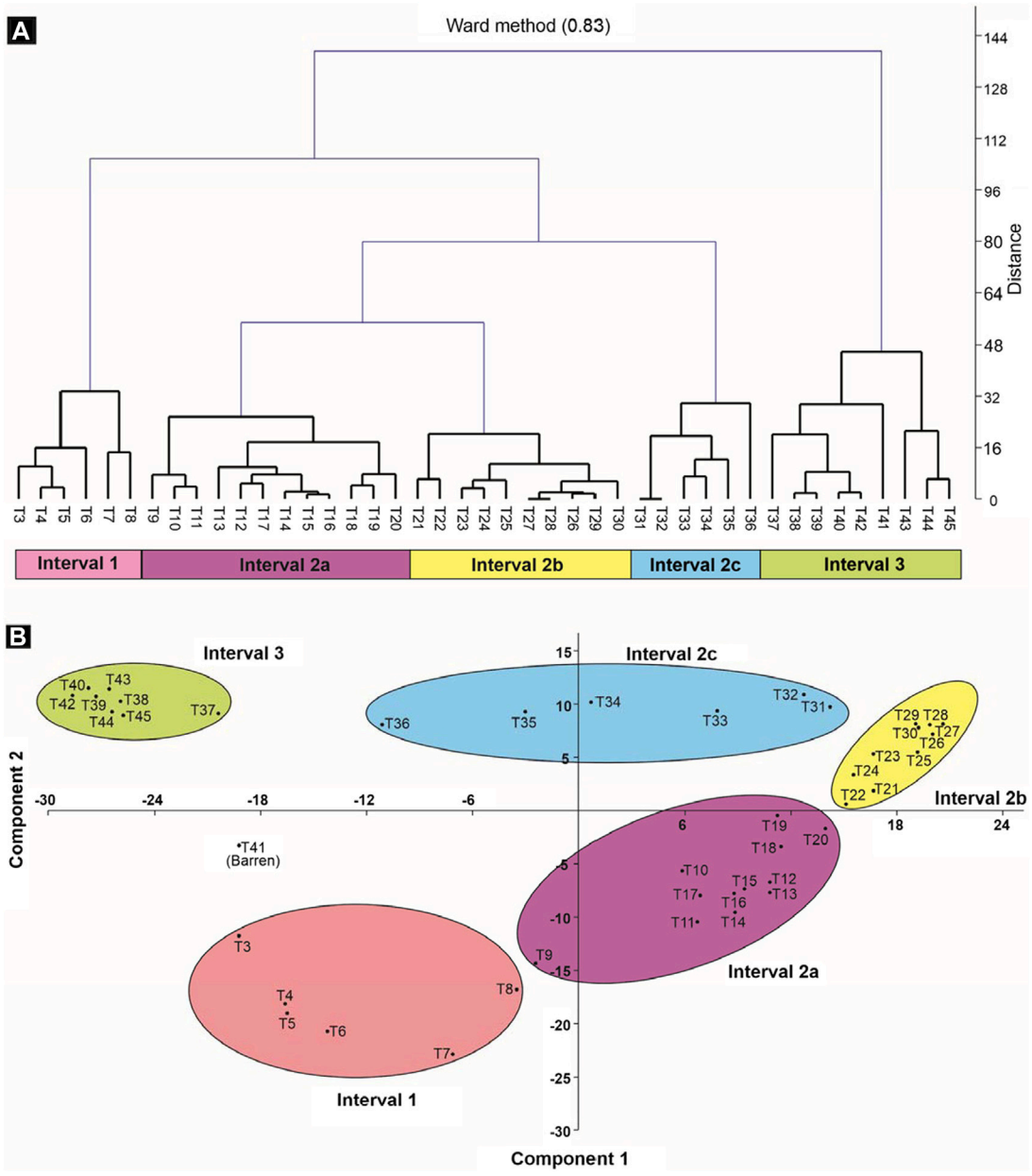

FIGURE 6
Quantitative analyses. Two analyses were used to define intervals in the present study (Intervals 1–3), hierarchical clustering **(A)** and principal component analysis **(B)**.

but show increasing values, from 0.42% to 0.62% with an average value of 0.55% (Figure 7).

4.5.2.3 Subinterval 2c (samples 31–36; P2–P3a)

In Subinterval 2c, six species make up 77% of the total planktic foraminiferal population, *P. varianta* (18.7%), *Subbotina triloculinoides* (16%), *P. pseudobulloides* (13.1%), *Praemurica uncinata* (12.7%), *Praemurica inconstans* (8.4%) and *Praemurica trinidadensis* (8.2%) (Figure 3). In terms of the genera, *Parasubbotina* (32.3%), *Praemurica* (29.3%) and *Subbotina* (26.9%) make up 88.5% of the total planktic foraminiferal population (Figure 7). Of the six most abundant species, four species show decreasing trends, *P. varianta* (from 16.3% to 6.1%; average 16.7%), *S. triloculinoides* (from 25% to 6.1%; average 14.6%), *P. pseudobulloides* (from 18.5% to 4.1%; average 11.7%) and *Pr. trinidadensis* (from 10.9% to 4.1%; average 7.6%); an increasing trend is noted for *Pr. uncinata* (from 3.8% to 18.4%; average 13.5%) and *Pr. inconstans* (from 10.9% to 12.2%; average 9%) (Figure 3). The subinterval is also marked by decreasing values of thermocline dwellers from 74% to 33% (average 62%), whereas both mix-layer dwellers (from 26% to 35%; average: 30%) and mix-layer with photosymbionts (from 0% to 33%; average: 30%) show increasing values (Figure 7). The cool water species (of *Parasubbotina* and *Subbotina*) dramatically decrease from 70% to 31% with an average

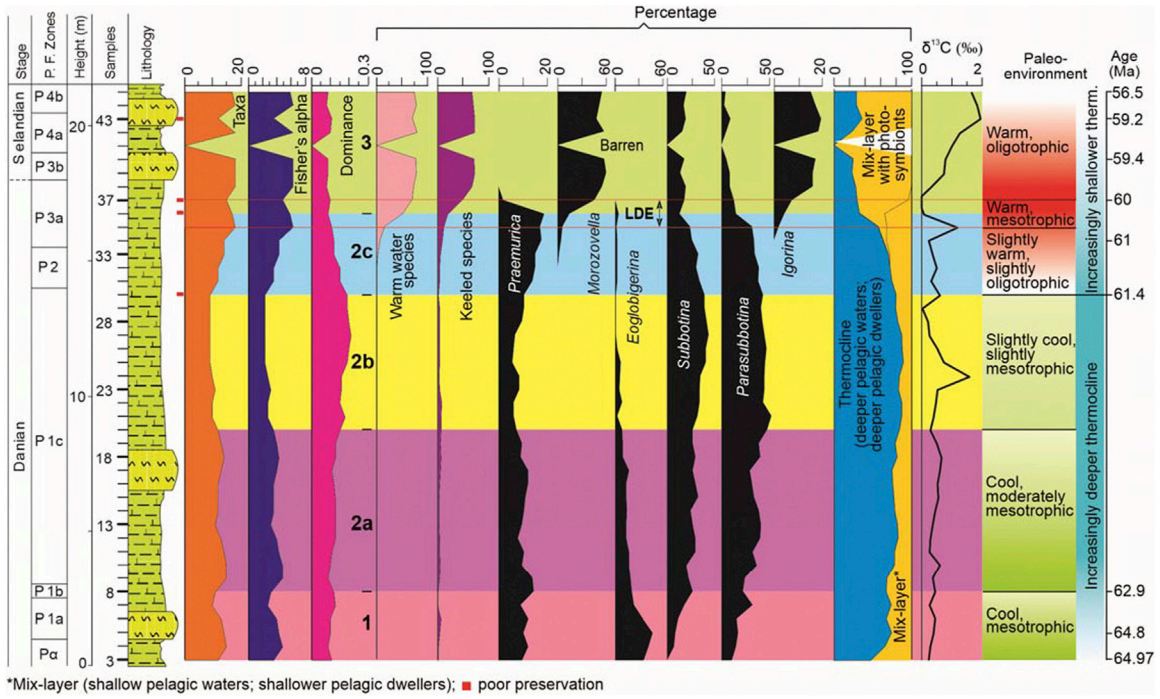

FIGURE 7
Proxies used to infer Danian–Selandian paleoenvironment. The proxies include species diversity (number of taxa, Fisher's α and species dominance), relative abundances of warm water species, keeled species, *Praemurica*, *Morozovella*, *Eoglobigerina*, *Subbotina*, *Parasubbotina*, *Igorina,* and categorization of planktic foraminiferal species bae on their depth preferences (mix-layer with photosymbionts, mix-layer and thermocline dwellers), $\delta^{13}C$ and inferred paleoenvironment based on these aforementioned proxies (see text for further explanation).

value of 57%; the warm water species show a corresponding increase, from 0 to 52 (average 13) (Figure 7). The relative abundance of keeled species marks their appearance and shows an increasing trend from 4.7% to 20.4% with an average value of 10% (Figure 7). The Subinterval 2c is also marked by increasing values of species diversity (the number of taxa increased from base to top, from 12 to 17; average 15; Fisher's α from 3.6 to 5.9; average 4.7) with decreasing values for species dominance (from 0.15 to 0.09; average 0.12) (Figure 7). The $\delta^{13}C$ values remain low and decreases from 0.33% to 0.10% with an average value of 0.46% (Figure 7).

4.5.2.4 Latest Danian Event (LDE, ~62.2 Ma)

In the present study, samples 35–37 (i.e., at the top of Subinterval 2c) mark the Latest Danian Event (LDE) (see Table 2; Figure 7) and are marked by the increased abundance of *Morozovella* (*M. praeangulata*, *M. angulata,* and *Morozovella conicontruncata*), reduction in *Parasubbotina* (particularly of *P. varianta*), *Subbotina* (particularly of *S. triloculinoides* and *S. cancellata*), *Praemurica* (*Pr. trinidadensis*, *Pr. inconstans* and *Pr. uncinata*) and *Globanomalina* (*G. ehrenbergi* and *G. compressa*), the emergence of *Igorina* (of *I. pusilla*) and *Acarinina* (*Acarinina hansbollii* and *A. strabocella*) and the final disappearance of *Eoglobigerina* (*Igorina spiralis*). The genus *Praemurica* disappears just after the LDE (see Table 1 and Figure 7). LDE is also marked by a dramatic decline in $\delta^{13}C$ values (i.e., a negative $\delta^{13}C$ excursion; from 1.19 to −0.10%), in Thermocline (from 57% to 30%) and mix-layer (32%–4%) dwellers, and the increased relative abundances of mix-layer with photosymbionts dwellers (from 11% to 66%), warm water (from 17% to 70%) and keeled species (from 12% to 50%), with decreased species diversity values (Fisher's α and the number of taxa; from 6.4 to 4.9 and 18 to 15, respectively); species dominance remains low (from 0.11 to 0.10) (see Table 1; Figure 7).

4.5.2.5 Interval 3 (samples 37–45; P3a–P4b)

In Interval 3, nine species make up 77% of the total planktic foraminiferal population, *M. angulata* (16.4%), *M. conicontruncata* (13%), *Morozovella apanthesma* (9.3%), *M. occlusa* (8.8%), *I. pusilla* (8.5%), *I. albeari* (6.6%), *A. hansbollii* (5.4%), *S. velascoensis* (5.2%) and *S. triangularis* (4.2%) (Figure 3). In terms of the genera, *Morozovella* (52.7%), *Subbotina* (16%), and *Igorina* (15.3%) make up 84% of the total planktic foraminiferal population (Figure 7). Of the nine most abundant species, four species show increasing values, *M. apanthesma* (from 0% to 12.5%; average 6.7%), *M. occlusa* (from 0% to 9.7%; average 8%), *Subbotina velascoensis* (from 0% to 9.7%; average 8%) and *I. albeari* (from 0% to 2.8%; average 4.9%), whereas the other five species show decreasing values, *M. angulata* (from 19.6% to 16.7%; average 15.4%), *A. hansbollii* (from 10.9% to 0%; average 3.5%), *M. conicontruncata* (from 6.5% to 2.8%; average 8.7%), *I. pusilla* (from 6.5% to 5.6%; average 6.7%), and *S. triangularis* (from 5.1% to 2.8%; average 3.8%) (Figure 3).

Interval 3 is also marked by increasing values of mix-layer with photosymbionts species, from 66% to 71% (average 64%), and slightly decreasing values of Thermocline dwellers, from 29.7% to

TABLE 2 Changes in proxies and species composition noted across the Latest Danian Event (LDE).

Age (Wade et al., 2011)			61	61	60				59.4
PF Zone		P3	P2	P3a				P3b	
Interval/Subinterval		2c					3		
Event					**LDE**				
Sample No.		T32	T33	T34	T35	T36	T37	T38	T39
$\delta^{13}C$ (‰)		0.50	0.38	0.26	1.19	0.10	−0.10	0.34	0.74
Taxa		12	14	14	18	17	15	18	18
Fisher alpha		3.6	4.4	4.4	6.4	5.9	4.9	6.4	6.4
Dominance		0.15	0.12	0.12	0.11	0.09	0.10	0.08	0.09
Evenness		0.68	0.72	0.72	0.67	0.83	0.78	0.79	0.77
% Warm water species			3	7	17	52	70	73	78
Keeled		5	6	9	12	20	50	68	73
% Thermocline		72	70	63	57	33	30	28	23
% Mix-layer with photosymbionts			2	4	11	33	66	72	77
% Mix-layer		28	28	33	32	35	4		
Morozovella praeangulata	Survivor		1.8	2.9	2.7	4.1	15.9	5.5	4.7
Morozovella angulata	Survivor			1.3	2.1	6.1	19.6	14.6	16.4
Morozovella conicontruncata	LDE-emergence				0.9	4.1	6.5	13.2	13.1
Morozovella occlusa	Post-LDE emergence							8.3	9.5
Morozovella apanthesma	Post-LDE emergence							8.4	9.3
Morozovella velascoensis	Post-LDE emergence							1.0	2.7
Parasubbotina varianta	Survivor	18.9	17.9	22.4	18.5	6.1	6.5	3.2	3.2
Parasubbotina pseudobulloides	LDE-Disappearance	17.2	14.4	8.4	7.9	4.1	2.2		
Parasubbotina variospira	LDE-emergence				2.3	4.1	2.9	5.0	4.9
Subbotina triloculinoides	Survivor	22.9	17.9	8.6	6.8	6.1	5.1	5.0	3.8
Subbotina cancellata	Survivor	2.9	5.4	8.4	7.9	4.1	6.5	4.0	2.4
Subbotina triangularis	Survivor		4.1	7.3	6.8	2.0	5.1	5.5	3.5
Subbotina velascoensis	Post-LDE emergence							3.7	3.7
Praemurica trinidadensis	LDE-Disappearance	11.5	8.0	6.7	4.2	4.1			
Praemurica inconstans	LDE-Disappearance	8.7	8.0	7.3	6.8	12.2	2.2		
Praemurica uncinata	LDE-Disappearance	7.6	12.0	18.5	21.0	18.4	2.2		
Igorina albeari	Post-LDE emergence							6.6	6.6
Igorina pusilla	LDE-emergence				1.6	4.1	6.5	8.4	8.3
Acarinina hansbollii	LDE-emergence				3.4	4.1	10.9	5.0	4.9
Acarinina strabocella	LDE-emergence					10.2	6.5	1.0	1.0
Globanomalina ehrenbergi	Survivor	1.0	1.4	1.7	1.6	2.0	1.4	0.8	0.8
Globanomalina compressa	LDE-Disappearance	3.1	1.9	2.1	2.0				
Globanomalina imitata	LDE-Disappearance	1.0	1.1	1.3	1.3				
Eoglobigerina spiralis	LDE-Disappearance	2.6	3.5	2.8	2.1	4.1			

29.2% (average 25%) (Figure 7). The cool water species (of *Parasubbotina* and *Subbotina*) show decreasing values from 28.3% to 23.6% with an average value of 21%; the warm water species show corresponding increasing values, from 70 to 75 (average 64) (Figure 7). The relative abundance of keeled species shows increasing values from 50% to 68%, averaging 61% (Figure 7). Interval 3 is also marked by increasing values of species diversity (number of taxa from 15 to 17; average 15; Fisher's α from 4.9 to 5.9; average 5.2) and decreasing values for species dominance (from 0.10 to 0.09; average 0.08) (Figure 7). The $\delta^{13}C$ values remain low but show increasing values, from 0.34% to 1.68% with an average of 1.06% (Figure 7).

5 Discussion

5.1 Paleoecological and paleoceanographic interpretations

The Pα–P1b zones (64.97–62.9 Ma; Interval 1; samples 3–8) are characterized by the dominance of thermocline dweller *Eoglobigerina* (36%: consisting of *E. eobulloides*, *E. edita* and *E. simplicissima*) (Figures 3, 7). The thermocline dwellers inhabit the deeper segments of the water column (e.g., thermocline), indicating the presence of a deeper thermocline, reduced stratification and/or eutrophic conditions (Bornemann et al., 2021) (see Table 1 for species habitat categorization). The other dominant taxa, *Praemurica* (20.4%: *Pr. taurica* and *Pr. pseudoinconstans*) prefers cooler waters (Guasti, 2005 and references therein); globally, the genus is well-documented to have disappeared just before the advent of the warm hypothermal Lower Danian Event (LDE: Berggren and Norris, 1997; Olsson et al., 1999; Jehle et al., 2015; 2019; Bornemann et al., 2021) (Figure 7). Cool surface waters are also supported by the presence of *Chiloguembelina* (*C. morsei*; 3.3%), *Globanomalina* (*G. archeocompressa* and *G. planocompressa*) and *Subbotina* (*S. triloculinoides* and *S. trivialis*; 7%) (see Boersma and Premoli Silva, 1983; Shackleton, 1985; Pearson et al., 1993; Van Eijden, 1995; Kelly et al., 1996; Lu et al., 1998; Quillévéré and Norris, 2003; Guasti, 2005) (Figure 7). Additionally, the warmest surface water temperatures are generally recorded by *Guembelitria* (Boersma and Premoli Silva, 1983) which is absent in the present study (Figure 7). The presence of the subsurface-dweller, *Parasubbotina* (14.4%: *P. moskvini* and *P. pseudobulloides*), is suggestive of mesotrophic conditions (Berggren and Norris, 1997; Olsson et al., 1999; Guasti, 2005; Jehle et al., 2015); the abundance of *Parasubbotina* slightly increases in the planktic foraminiferal Zone P1a–P1b (samples 5–8) (Figure 7). The low $\delta^{13}C$ values (between 0.26% and 0.47%) during the entire interval is also suggestive of increased surface water fertility.

Thus, the present data suggest that during the planktic foraminiferal Zone Pα (samples 3–4), moderately shallow and eutrophic conditions prevailed with cool surface waters and with a shallow thermocline, whereas for the succeeding P1a–P1b zones (samples 5–8), similar conditions are noted, but with reduced productivity (i.e., slight mesotrophic conditions) and a somewhat deeper thermocline and reduced stratification (Figure 7). This duration is marked by low species diversity (11–15 taxa) but also with low species dominance and high evenness suggesting that increased productivity (low $\delta^{13}C$ values and relative abundances of mesotrophic taxa, *Chiloguembelina* and *Woodringina*: 3.3% and 15.1%, respectively) did not severely affect the fauna, that would have otherwise caused oxygen-depleted conditions (Figure 7). Additionally, moderate to good preservation of samples also suggest that dissolution did not play a major role in altering species composition (Figure 7).

The P1a Subzone also records the Dan-2 event (samples 6–7; Figure 7). This event is considered a transient hyperthermal episode that records a shift in carbon reservoirs and ocean warming in the northwestern and southeastern sectors of the Atlantic Ocean and is marked by environmental perturbation resulting in enhanced eutrophication of the sea surface waters and carbonate dissolution (Coccioni et al., 2010). It has been suggested that as the environmental conditions became more stable after the K–Pg event, *Guembelitria* retreated and vacated its niche to other ecological generalists such as the low-oxygen tolerant small biserial taxa (*Heterohelix*, *Chiloguembelina*, *Woodringina*, and *Zeuvigerina*), that slightly increased in abundance during the Dan-C2 event (Coccioni et al., 2010).

In the present study, during the Dan-C2 event, only *Woodringina* (9.5%) and *Chiloguembelina* (2.2%) are recorded, and both are also cool water forms (Boersma and Premoli Silva, 1983). *Guembelitria* and *Heterohelix* have not been recorded in the present study, whereas *Zeuvigerina* only occurs at the top of the studied section (samples 44–45). *Eoglobigerina eobulloides* dominates during this event and is associated with low species diversity (the average values of Fisher's α number of taxa are 11.5 and 3.4, respectively) and low species dominance (average value: 0.11), suggesting that increased mesotrophy did not result in stressed or low-oxygen conditions, during this transient interval.

Keller (2014) noted that the last Deccan phase 3 began at the base of C29N and was accompanied by the extinction of *P. eugubina*. In the present study, only samples 3 to 4 have yielded *P. eugubina*. Hence, in our present study, samples 5–8 of Interval 1 (Figure 7) correspond with Phase 3 of the Deccan volcanism. Keller (2014) noted that the early Danian zones P0 and P1a record a high-stressed environment with the upper part of P1a registering improved conditions but marked by low species diversity (12–15 number of taxa). In the present study, species diversity also remains low (between 10 and 15; average: 12.5), but species dominance is also low (averaging 0.11), suggesting a more or less equitable paleoenvironment rather than stressed conditions (see Figure 7). Additionally, the dominant early Danian species of *Guembelitria cretacea*, suggestive of high-stress conditions (Keller, 2014) has not been recorded in the present study; the presence of low-oxygen tolerant taxa *Woodringina* (3.6%) and *Chiloguembelina* (1.4%) are noted, but in only in lower abundances, suggesting the absence of stressed conditions.

The planktic foraminiferal zones P1b–P1c (subintervals 2a–2b; samples 9–30) exhibit a major shift in species composition, a change from the dominance of *Eoglobigerina* (36.1%; *E. eobulloides*: 13.2%) to *Subbotina–Parasubbotina* (*S. triloculinoides* and *P. pseudobulloides*, 20.5% each). *Parasubbotina* and *Subbotina* (59%) are considered cool surface water species and deep thermocline dwellers, suggesting enhanced and stable water column stratification and meso-to oligotrophic conditions (Boersma and Premoli Silva, 1983; Boersma and Premoli Silva, 1991; Pearson et al., 1993; Norris,

1996; Berggren and Norris, 1997) (Figure 7). However, Bornemann et al. (2021) considered them as mesotrophic, subsurface taxa; lower $\delta^{13}C$ values throughout the interval also suggests increased productivity. In the present study, during the LDE hypothermal event, both *Parasubbotina* and *Subbotina* decreased dramatically, suggesting their preference for cooler mesotrophic waters (see also Guasti, 2005 and references therein); low $\delta^{13}C$ values throughout the interval also supports mesotrophic conditions (Figure 7). It must be noted that the upper ocean warming produces a more stable water column which, in turn, inhibits primary productivity (surface water fertility). Thus, increased stratification inhibits surface water productivity, whereas decreased stratification promotes it (Behrenfeld et al., 2006; Polovina et al., 2008).

Thus, for Subinterval 2a, the lower part of Subzone P1c (samples 9–20), cooler surface waters and moderate mesotrophic conditions are noted (Figure 7).

Subinterval 2b (the upper part of Subzone P1c; samples 21–30) displays a reduction in the relative abundance of *Praemurica*, a genus that has been noted to prefer cooler waters (Guasti, 2005 and references therein). In the present study, *Praemurica* shows its lowest relative abundance in Subinterval 2b with maximum abundance during the mesotrophic hypothermal LDE event, suggesting its preference more for nutrient availability rather than temperature (Figure 7). Hence, for Subinterval 2b only slightly mesotrophic conditions are suggested, as also demonstrated by somewhat higher $\delta^{13}C$ values (Figure 7).

The planktic foraminiferal Zone P2 to the lower part of Subzone P3a (i.e., Subinterval 2c; samples 31–36) are transitionary times, where *Praemurica* reaches its maximum relative abundance, 29.3% (represented by *Pr. uncinata*, 12.7%; *Pr. inconstans*, 8.4%, and *Pr. trinidadensis*, 8.2%) with the corresponding rise of *Morozovella* (FO at sample 33), *Acarinina* (FO at sample 35) and *Igorina* (FO at sample 35) (Figure 7). Birch et al. (2012) noted that *P. uncinata* shared the warm surface mixed-layer niche with *M. praeangulata* (a strongly symbiotic species) that, in the present study, makes up a minor fraction (1.5%; FO at sample 34) of the total population suggesting warming of the surface waters at the end of planktic foraminiferal Zone P2 (sample 33) (Figure 7). Additionally, the stable isotope measurements of *Morozovella*, *Acarinina* and *Igorina* typify food-poor oligotrophic pelagic environments at low latitudes (Norris, 1996; D'Hondt and Zachos, 1998; Coxall et al., 2006; Fuqua et al., 2008; Birch et al., 2012). A similar pattern of increased abundances and diversity of *Morozovella*, *Acarinina* and *Igorina* was also observed in other sections spanning the Danian-Selandian transition, as in the South Atlantic Ocean (Coxall et al., 2006; Birch et al., 2012), North Atlantic and Pacific Oceans (Berggren and Norris, 1997), and sections in Spain (Arenillas and Molina, 1995; 1997); all suggestive of a well stratified water column and oligotrophic conditions. The warming of surface waters and shallowing of the thermocline are also corroborated by the rise of mix-layer and mix-layer with photosymbionts dwellers and the corresponding decline of thermocline ones, i.e., the deeper pelagic dwellers (Figure 7). This subinterval is also marked by increased species diversity (Fisher's α and number of taxa), and lowered species dominance suggesting equitable conditions (Figure 7).

The planktic foraminiferal Zone P3a (and the upper part of Subinterval 2c) marks the Latest Danian Event (LDE, samples 35–37; 60–61 Ma) (Figure 7). In the present study, LDE is constrained on the lower side by the LO of *M. angulata* (sample 34; 61 Ma; Wade et al., 2011) and on the upper side, by the LO of *I. albeari* (sample 38; 60 Ma; Wade et al., 2011) (see also Table 2). In the present study, the LDE is marked by a dramatic decline in $\delta^{13}C$ values (i.e., a negative $\delta^{13}C$ excursion), Thermocline (*Parasubbotina* and *Subbotina*), and mix-layer (particularly *Praemurica*) dwellers, and an abrupt increase in mix-layer with photosymbiont dwellers, warm water (*Morozovella* and *Igorina*) and keeled species (see Table 2; Figure 7).

Globally, also, the LDE is characterized by a prominent negative $\delta^{13}C$ excursion in different marine settings like the southern Tethyan shelf (Egypt; Bornemann et al., 2009), the northern Tethys (Bjala, Bulgaria; Dinarès-Turell et al., 2012), the eastern North Atlantic (Zumaia, Spain; Dinarès-Turell et al., 2010), and the Pacific Ocean (Westerhold et al., 2011; see also Bornemann et al., 2021). As with other Paleogene hyperthermals (such as the PETM), the negative $\delta^{13}C$ excursion has been attributed to the addition of huge amounts of $\delta^{13}C$ depleted carbon to the ocean and atmosphere. The coincident surface water warming has been explained either by the possibility of high atmospheric greenhouse gas concentrations similar to that noted for the PETM or increased insolation due to the orbital constellation (Pc40510; Dinarès-Turell et al., 2014) i.e., changes of orbital parameters resulting in insolation changes on shorter time-scales during the upper Chron C27n (see also Bornemann et al., 2021). Additionally, the LDE falls within a time interval that shows an increased activity of the North Atlantic Igneous Province, and oceanic spreading rates and volcanic activity along the SE Greenland margin (Sinton and Duncan, 1998; Westerhold et al., 2008). Evaluation of all the aforementioned mechanisms is beyond the scope of the present study, but the coincidence of surface water warming and increased mesotrophy is also noted in the present study (Figure 7). Additionally, as at Site 1262 (eastern South Atlantic Ocean), during the LDE, an increased abundance of *Morozovella* and *Igorina* (see Figure 7) has also been noted to suggest surface-water warming (see Jehle et al., 2019).

Thus, based on available and present data, the LDE in the present study is marked by increased mesotrophy (negative $\delta^{13}C$ excursion), enhanced stratification of the upper water column, and transient surface water warming as indicated by the increased relative abundances of surface-dwelling planktic foraminifera, mix-layer, and mix-layer with photosymbionts dwellers. Increased mesotrophy also resulted in reduced species diversity, as evidenced by reduced values of Fisher's α and the number of taxa (Figure 7).

The upper part of planktic foraminiferal subzones P3b to P4b (samples 39–45; 60–56.5 Ma) is marked by the dominance of *Morozovella*, *Acarinina*, *Igorina*, warm water species, mix-layer with photosymbionts dwellers, and high values of $\delta^{13}C$, suggestive of warm, oligotrophic conditions (Norris, 1996; D'Hondt and Zachos, 1998; Coxall et al., 2006; Fuqua et al., 2008; Birch et al., 2012). Both *Morozovella* and *Acarinina* have been noted to diversify during the globally warm Paleocene–Eocene Thermal Maximum (PETM), both in open ocean ODP sites and in the marginal Tethys (see also Kelly et al., 1996; Guasti and Speijer, 2008; Hewaidy et al., 2020), corroborating a phase of surface water warming for Interval 3 of the present study. Coxall et al. (2006) suggested that the timing of radiation in *Morozovella* and other

muricate algal symbionts genera (such as *Acarinina* and *Igorina*) represent the diversification of oligotrophic specialists as an organic flux to the deep ocean fully recovered, stripping of nutrients from the surface ocean resumed, and specialization to low food availability became a selective advantage (see also Shackleton, 1985; Pearson et al., 1993; D'Hondt et al., 1994; Van Eijden, 1995; Kelly et al., 1996; Lu et al., 1998; Quillévéré and Norris, 2003; Guasti et al., 2005). These warm and oligotrophic conditions also favored the highest species diversity values (of Fisher's α and number of taxa), and lowest species dominance suggesting equitable conditions (Figure 7).

6 Conclusion

- A total of 43 samples from the Themed section (El Themed village in East Central Sinai) spanning zones *P. eugubina* (Pα; 64.97–64.8 Ma) to the *A. subsphaerica* (P4b; 59.2–56.5 Ma) are studied to infer the paleoenvironment across the Danian–Selandian duration.
- Four biozones are recorded, *P. eugubina* (Pα) Zone, *E. edita* (P1) Zone (with three subzones, *P. pseudobulloides*, P1a, *S. triloculinoides*, P1b, and *G. compressa*, P1c), *Pr. uncinata* (P2) Zone, *M. angulata* (P3) Zone (this includes two subzones, *I. pusilla*, P3a, *I. albeari*, P3b), *G. pseudomenardii* (P4) Zone (with two subzones, *G. pseudomenardii*/*P. variospira*, P4a, and *A. subsphaerica*, P4b).
- Two $\delta^{13}C$ events are identified, Dan-C2 and Latest Danian Event (LDE); an additional two are suggested, Lower Chron 29n (L. C29n) and Middle Chron 27r (M. C27r). However, for the latter two, more data is needed to characterize them thoroughly.
- During Pα (samples 3–4), moderately shallow and eutrophic conditions prevailed with cool surface waters and a shallow thermocline. For P1a–P1b subzones (samples 5–8), mesotrophic conditions and a somewhat deeper thermocline with reduced stratification have been noted.
- The Dan-2 event (samples 6–7) is marked by the dominance of *E. eobulloides* with cool waters and mesotrophic conditions.
- During P1b–P1c (subintervals 2a–2b; samples 9–30), a major shift in species composition, a change from the dominance of *Eoglobigerina* (*E. eobulloides*) to *Subbotina–Parasubbotina* (*S. triloculinoides* and *P. pseudobulloides*).
- During Subinterval 2a, cooler surface waters and moderate mesotrophic conditions are noted, and for Subinterval 2b, slightly mesotrophic conditions with cooler waters.
- During P2 to the lower part of P3a (i.e., Subinterval 2c; samples 31–36) are transitionary, marked by the maximum abundance of *Praemurica* and the rise of *Morozovella*, *Acarinina,* and *Igorina.* Warming surface waters and the thermocline shallowing with increased oligotrophic conditions are noted.
- During P3a (and the top of Subinterval 2c) marks the Latest Danian Event (LDE, samples 35–37; 60–61 Ma). The LDE is marked by a negative $\delta^{13}C$ excursion, a decline in values of thermocline and mix-layer dwellers, and an abrupt increase in mix-layer with photosymbiont dwellers, and warm waters suggesting increased mesotrophy, enhanced stratification and transient surface water warming.
- During the upper part of planktic foraminiferal zones P3b to P4b (samples 39–45; 60–56.5 Ma), the dominance of *Morozovella*, *Acarinina,* and *Igorina* are noted with warm water species, mix-layer with photosymbionts dwellers, and high values of $\delta^{13}C$, suggestive of warm, oligotrophic conditions.

Data availability statement

The datasets presented in this study can be found in online repositories. The names of the repository/repositories and accession number(s) can be found in the article/supplementary material.

Author contributions

All authors listed have made a substantial, direct, and intellectual contribution to the work and approved it for publication.

Acknowledgments

We sincerely thank Dr. Hema Achyuthan (Frontiers in Earth Science Associate Editor) and the reviewers for their time, constructive comments, and suggestions that significantly improved the manuscript. The financial support of Research Supporting Project number (RSP2023R139), King Saud University, Riyadh, Saudi Arabia, is also acknowledged. The authors acknowledge the UiT, the Arctic University of Norway, for open access funding.

Conflict of interest

The authors declare that the research was conducted in the absence of any commercial or financial relationships that could be construed as a potential conflict of interest.

Publisher's note

References

Allan, J., and Matthews, R. (1982). Isotope signatures associated with early meteoric diagenesis. *Sedimentology* 29, 797–817. doi:10.1111/j.1365-3091.1982.tb00085.x

Arenillas, I., and Molina, E. (1995). Analisis cuantitativo de los foraminiferos planctonicos de Paleoceno en zumaya: Implicaciones paleoambientales y eventos paleoceanograficos. *Geogaceta* 17, 23–26.

Arenillas, I., and Molina, E. (1997). Análisis cuantitativo de los foraminíferos planctónicos del Paleoceno de Caravaca (Cordilleras Béticas): Cronoe-stratigrafía, bioestratigrafía y evolución de las asociaciones. *Rev. Española Paleontol.* 12, 207–232.

Aze, T., Ezard, T. H. G., Purvis, A., Coxall, H. K., Stewart, R. M., Wade, B. S., et al. (2011). A phylogeny of Cenozoic macroperforate planktonic foraminifera from fossil data. *Biol. Rev.* 86, 900–927. doi:10.1111/j.1469-185x.2011.00178.x

Barazi, N., and Kuss, J. (1987). Southernmost outcrops of marine lower Tertiary carbonate rocks in NE-Africa (Gebel Abyad, Sudan). *Geol. Rundsch.* 76, 529–537. doi:10.1007/BF01821090

Barnet, J. S. K., Littler, K., Kroon, D., Leng, M. J., Westerhold, T., Röhl, U., et al. (2017). A new high-resolution chronology for the late maastrichtian warming event: Establishing robust temporal links with the onset of deccan volcanism. *Geology* 46, 147–150. doi:10.1130/g39771.1

Barnet, J. S. K., Littler, K., Westerhold, T., Kroon, D., Leng, M. J., Bailey, I., et al. (2019). A high-fidelity benthic stable isotope record of late cretaceous-early eocene climate change and carbon cycling. *Paleoceanogr. Paleoclimatol* 34, 672–691. doi:10.1029/2019pa003556

Bazeen, Y. S., Hewaidy, A. G. A., Samir, A., Moneer, E. S. M., Abd El-Moghny, M. W., and Ayyad, H. M. (2023). Sequence stratigraphy of the Paleocene succession in the kharga oasis, western Desert, Egypt: Insights from microplankton biostratigraphy and benthic foraminifer paleoenvironments. *Palaeoworld*. doi:10.1016/j.palwor.2023.01.005

Behrenfeld, M. J., O'Malley, R. T., Siegel, D. A., McClain, C. R., Sarmiento, J. L., Feldman, G. C., et al. (2006). Climate-driven trends in contemporary ocean productivity. *Nature* 444 (7120), 752–755. doi:10.1038/nature05317

Berggren, W. A., Aubry, M.-P., van Fossen, M., Kent, D. V., Norris, R. D., and Quillévéré, F. (2000). Integrated Paleocene calcareous plankton magneto-biochronology and stable isotope stratigraphy: DSDP site 384 (NW Atlantic Ocean). *Palaeogeogr. Palaeoclimatol. Palaeoecol.* 159, 1–51. doi:10.1016/s0031-0182(00)00031-6

Berggren, W. A., and Norris, R. D. (1997). Biostratigraphy, phylogeny and systematics of Paleocene trochospiral planktic foraminifera. *Micropaleontology* 43 (1), 1–116. doi:10.2307/1485988

Berggren, W. A., and Ouda, K. (2003). "Upper paleocene–lower eocene planktonic foraminiferal biostratigraphy of the dababiya section, upper nile valley (Egypt)," in *The upper paleocene–lower eocene of the upper nile valley: Part 1, stratigraphy*. Editors K. Ouda and M.-P. Aubry, 61–92. Micropaleontology.

Birch, H. S., Coxall, H. K., and Pearson, P. N. (2012). Evolutionary ecology of early Paleocene planktonic foraminifera: Size, depth habitat and symbiosis. *Paleobiology* 38 (3), 374–390. doi:10.1666/11027.1

Boersma, A., and Premoli Silva, I. (1991). Distribution of Paleogene planktonic foraminifera analogies with Recent? *Palaeogeogr. Palaeoclimatol. Palaeoecol.* 83, 29–47. doi:10.1016/0031-0182(91)90074-2

Boersma, A., and Premoli Silva, I. (1983). Paleocene planktonic foraminiferal biogeography and the paleooceanography of the Atlantic Ocean. *Micropaleontology* 29 (4), 355–381. doi:10.2307/1485514

Bornemann, A., Jehle, S., Lägel, S., Deprez, A., Petrizzo, M. R., and Speijer, R. P. (2021). Planktic foraminiferal response to an early Paleocene transient warming event and biostratigraphic implications. *Int. J. Earth Sci.* 110, 583–594. doi:10.1007/s00531-020-01972-z

Bornemann, A., Schulte, P., Sprong, J., Steurbaut, E., Youssef, M., and Speijer, R. P. (2009). Latest Danian carbon isotope anomaly and associated environmental change in the southern Tethys (Nile Basin, Egypt). *J. Geol. Soc.* 166, 1135–1142. doi:10.1144/0016-76492008-104

Coccioni, R., Frontalini, F., Bancalà, B., Fornaciari, E., Jovane, L., and Sprovieri, M. (2010). The Dan-C2 hyperthermal event at Gubbio (Italy): Global implications, environmental effects, and cause(s). *Earth Planet. Sci. Lett.* 297 (1), 298–305. doi:10.1016/j.epsl.2010.06.031

Coxall, H. K., D'Hondt, S., and Zachos, J. C. (2006). Pelagic evolution and environmental recovery after the Cretaceous-Paleogene mass extinction. *Geology* 34, 297–300. doi:10.1130/g21702.1

Coxall, H. K., Pearson, P. N., Shackleton, N. J., and Hall, M. (2000). Hantkeninid depth adaptation: An evolving life strategy in a changing ocean. *Geology* 28, 87–90. doi:10.1130/0091-7613(2000)028<0087:hdaael>2.3.co;2

D'Hondt, S., and Zachos, J. C. (1998). Cretaceous foraminifera and the evolutionary history of planktic photosymbiosis. *Paleobiology* 24, 512–523. doi:10.1017/s0094837300020133

D'Hondt, S., and Zachos, J. C. (1993). On stable isotopic variation and earliest Paleocene planktonic foraminifera. *Paleoceanography* 8, 527–547. doi:10.1029/93pa00952

D'Hondt, S., Zachos, J. C., and Schultz, G. (1994). Stable isotopic signals and photosymbiosis in Late Paleocene planktic foraminifera. *Paleobiology* 30 (3), 391–406. doi:10.1017/s0094837300012847

Dinarès-Turell, J., Pujalte, V., Stoykova, K., Baceta, J. I., and Ivanov, M. (2012). The palaeocene "top chron C27n" transient greenhouse episode: Evidence from marine pelagic atlantic and peri-tethyan sections. *Terra nova.* 24 (6), 477–486. doi:10.1111/j.1365-3121.2012.01086.x

Dinarès-Turell, J., Stoykova, K., Baceta, J. I., Ivanov, M., and Pujalte, V. (2010). High-resolution intra- and interbasinal correlation of the danian-selandian transition (early Paleocene): The bjala section (Bulgaria) and the selandian GSSP at Zumaia (Spain). *Palaeogeogr. Palaeoclimatol. Palaeoecol.* 297 (2), 511–533. doi:10.1016/j.palaeo.2010.09.004

Dinarès-Turell, J., Westerhold, T., Pujalte, V., Röhl, U., and Kroon, D. (2014). Astronomical calibration of the danian stage (early Paleocene) revisited: Settling chronologies of sedimentary records across the atlantic and Pacific oceans. *Earth Planet. Sci. Lett.* 405, 119–131. doi:10.1016/j.epsl.2014.08.027

Farouk, S., and El-Sorogy, A. (2015). Danian/Selandian unconformity in the central and southern Western Desert of Egypt. *J. Afr. Earth Sci.* 103, 42–53. doi:10.1016/j.jafrearsci.2014.12.002

Farouk, S. (2016). Paleocene stratigraphy in Egypt. *J. Afr. Earth Sci.* 113, 126–152. doi:10.1016/j.jafrearsci.2015.10.013

Fuqua, L. M., Bralower, T. J., Arthur, M. A., and Patzkowsky, M. E. (2008). Evolution of calcareous nannoplankton and the recovery of marine food webs after the Cretaceous-Paleocene mass extinction. *Palaios* 23, 185–194. doi:10.2110/palo.2007.p07-004r

Geological Survey of Egypt (1994). *Geological map of Sinai, Egypt (sheet no. 1 and 3), scale 1:250,000*. Geological Survey of Egypt.

Guasti, E. (2005). *Early Paleogene environmental turnover in the Southern Tethys as recorded by foraminiferal and organic-walled dinoflagellate cysts assemblages*. Ph.D. thesis. Universität Bremen, 203.

Guasti, E., and Speijer, R. P. (2008). <i>Acarinina multicamerata</i> n. sp. (foraminifera): A new marker for the paleocene–eocene thermal maximum. *J. Micropalaeontology* 27, 5–12. doi:10.1144/jm.27.1.5

Guasti, E., Speijer, R. P., Fornaciari, E., Schmitz, B., Kroon, D., and Gharaibeh, A. (2005). *Transient biotic change within the Danian–Selandian transition in Egypt and Jordan*. Chapter IV of Ph. D. E. Guasti, Early Paleogene environmental turnover in the Southern Tethys as recorded by foraminiferal and organic-walled dinoflagellate cysts assemblages. Universität Bremen, 75–110.

Hammer, Ø., Harper, D. A., and Ryan, P. D. (2001). PAST: Paleontological statistics software package for education and data analysis. *Palaeontol. Electron.* 4, 1–9.

Hewaidy, A. A., Farouk, S., and Bazeen, Y. S. (2019). Foraminiferal biostratigraphy and paleoenvironments of the danian-selandian succession at the kharga oasis, western Desert, Egypt. *Arab. J. Geosci.* 12, 133–217. doi:10.1007/s12517-019-4229-z

Hewaidy, A. A., Farouk, S., and Bazeen, Y. S. (2017). Sequence stratigraphy of the maastrichtian-paleocene succession at the Dakhla oasis, western Desert, Egypt. *J. Afr. Earth Sci.* 136, 22–43. doi:10.1016/j.jafrearsci.2016.11.028

Hewaidy, A. A., Farouk, S., and Bazeen, Y. S. (2020). Upper palaeocene – lower eocene succession of the kharga oasis, western Desert, Egypt: Foraminiferal biostratigraphy and sequence stratigraphy. *Geol. J.* 55, 4375–4397. doi:10.1002/gj.3674

Huber, B. T., and Boersma, A. (1994). Cretaceous origin of *Zeauvigerina* and its relationship to Paleocene biserial planktonic foraminifera. *J. Foraminifer. Res.* 24, 268–287. doi:10.2113/gsjfr.24.4.268

Jarvis, I., Lignum, J. S., Groecke, D. R., Jenkyns, H. C., and Pearce, M. A. (2011). Black shale deposition, atmospheric CO2 drawdown, and cooling during the Cenomanian-Turonian Oceanic Anoxic Event. *Paleoceanography* 26, Pa3201. doi:10.1029/2010pa002081

Jarvis, I., Mabrouk, A., Moody, R. T. J., and De Cabrera, S. C. (2002). Late Cretaceous (Campanian) carbon isotope events, sea-level change and correlation of the Tethyan and Boreal realms. *Palaeogeogr. Palaeoclimatol. Palaeoecol.* 188, 215–248. doi:10.1016/s0031-0182(02)00578-3

Jehle, S., Bornemann, A., Deprez, A., and Speijer, R. P. (2015). The impact of the latest danian event on planktic foraminiferal faunas at ODP site 1210 (shatsky rise, Pacific ocean). *PLoS ONE* 10 (11), e0141644. doi:10.1371/journal.pone.0141644

Jehle, S., Bornemann, A., Lägel, A. F., Deprez, A., and Speijer, R. P. (2019). Paleoceanographic changes across the latest danian event in the South Atlantic Ocean and planktic foraminiferal response. *Palaeogeogr. Palaeoclimatol. Palaeoecol.* 525, 1–13. doi:10.1016/j.palaeo.2019.03.024

Jenkyns, H. C., Gale, A. S., and Corfield, R. M. (1994). Carbon- and oxygen-isotope stratigraphy of the English Chalk and Italian Scaglia and its palaeoclimatic significance. *Geol. Mag.* 131, 1–34. doi:10.1017/s0016756800010451

Keller, G. (2014). Deccan volcanism, the chicxulub impact, and the end-cretaceous mass extinction: Coincidence? Cause and effect? *Geol. Soc. Am. Special Pap.* 505, 57–89.

Kelly, C. D., Bralower, T. J., Zachos, J. C., Premoli Silva, I., and Thomas, E. (1996). Rapid diversification of planktonic foraminifera in the tropical pacific (ODP site 865) during the late Paleocene thermal maximum. *Geology* 24 (5), 423–426. doi:10.1130/0091-7613(1996)024<0423:rdopfi>2.3.co;2

Krahl, G., Koutsoukos, E. A. M., and Fauth, G. (2017). Paleocene planktonic foraminifera from DSDP site 356, South Atlantic: Paleoceanographic inferences. *Mar. Micropaleontol.* 135, 1–14. doi:10.1016/j.marmicro.2017.07.001

Kroon, D., and Zachos, J. C. (2007). "Leg 208 synthesis: Cenozoic climate cycles and excursions," in Proceedings of the Ocean Drilling Program, College Station, TX (Ocean Drilling Program), 55. Scientific Results. doi:10.2973/odp.proc.sr.208.201.2007

Lu, G., Keller, G., and Pardo, A. (1998). Stability and change in Tethyan planktic foraminifera across the Paleocene–Eocene transition. *Mar. Micropaleontol.* 35, 203–233. doi:10.1016/s0377-8398(98)00018-8

Lu, G., and Keller, G. (1996). Separating ecological assemblages using stable isotope signals: Late Paleocene to early eocene planktic foraminifera, DSDP site 577. *J. Foraminifer. Res.* 26, 103–112. doi:10.2113/gsjfr.26.2.103

Macleod, N., and Keller, G. (1991). How complete are cretaceous/tertiary boundary sections? A chronostratigraphic estimate based on graphic correlation. *Geol. Soc. Am. Bull.* 103 (11), 1439–1457. doi:10.1130/0016-7606(1991)103<1439:hcactb>2.3.co;2

Monechi, S., Reale, V., Bernaola, G., and Balestra, B. (2013). The danian/selandian boundary at site 1262 (South Atlantic) and in the tethyan region: Biomagnetostratigraphy, evolutionary trends in fasciculiths and environmental effects of the latest danian event. *Mar. Micropaleontol.* 98, 28–40. doi:10.1016/j.marmicro.2012.11.002

Norris, R. D. (1996). Symbiosis as an evolutionary innovation in the radiation of Paleocene planktic foraminifera. *Paleobiology* 22 (4), 461–480. doi:10.1017/s0094837300016468

Obaidalla, N. A., El-Dawy, M. H., and Kassab, A. S. (2009). Biostratigraphy and paleoenvironment of the danian/selandian (D/S) transition in the southern Tethys: A case study from north Eastern Desert, Egypt. *J. Afr. Earth Sci.* 53, 1–15. doi:10.1016/j.jafrearsci.2008.07.004

Olsson, R. K., Hemleben, C., Berggren, W. A., and Huber, B. T. (1999). Atlas of Paleocene planktonic foraminifera. *Smithson. contribution Paleobiology* 85, 1–252. doi:10.5479/si.00810266.85.1

Pearson, P. N., Ditchfield, P. W., Singano, J., Harcourt-Brown, K. G., Nicholas, C. J., Olsson, R. K., et al. (2001). Warm tropical sea surface temperatures in the Late Cretaceous and Eocene epochs. *Nature* 413, 481–487. doi:10.1038/35097000

Pearson, P. N., Shackleton, N. J., and Hall, M. A. (1993). Stable isotope paleoecology of middle Eocene planktonic foraminifera and multispecies isotope stratigraphy, DSDP Site 523, South Atlantic. *J. Foraminifer. Res.* 23 (2), 123–140. doi:10.2113/gsjfr.23.2.123

Polovina, J. J., Howell, E. A., and Abecassis, M. (2008). Ocean's least productive waters are expanding. *Geophys. Res. Lett.* 35, L03618. doi:10.1029/2007GL031745

Punekar, J., Keller, G., Khozyem, H. M., Hamming, C., Adatte, T., Tantawy, A. A., et al. (2014). Late Maastrichtian-early Danian high-stress environments and delayed recovery linked to Deccan Volcanism. *Cretac. Res.* 49, 63–82. doi:10.1016/j.cretres.2014.01.002

Quillévéré, F., and Norris, R. D. (2003). "Ecological development of acarininids (planktonic foraminifera) and hydrographic evolution of Paleocene surface waters," in *Causes and consequences of globally warm climates in the early Paleogene*. Editors S. L. Wing, P. D. Gingerich, B. Schmitz, and E. Thomas (Boulder, Colorado: Geological Society of America Special Paper), 223–238.

Said, R. (1962). *The geology of Egypt*. Amsterdam: Elsevier, 377.

Salhi, I., Elamri, Z., Bazeen, Y. S., Ahmad, F., Mahmoudi, S., and Farouk, S. (2022). Planktonic foraminifera and stable isotopes of the upper Cenomanian-middle Turonian in central Tunisia: Implications for bioevents synchronicity and paleoenvironmental turnover. *Cretac. Res.* 138, 105291. doi:10.1016/j.cretres.2022.105291

Schmitz, B., Molina, E., and von Salis, K. (1998). The zumaya section in Spain: A possible global stratotype section for the selandian and thanetian stages. *Newsl. Stratigr.* 36, 35–42. doi:10.1127/nos/36/1998/35

Schmitz, B., Pujalte, V., Molina, E., Monechi, S., Orue-Etxebarria, X., Speijer, R. P., et al. (2011). The global stratotype sections and points for the bases of the selandian (middle Paleocene) and thanetian (upper Paleocene) stages at Zumaia, Spain. *Episodes* 34, 220–243. doi:10.18814/epiiugs/2011/v34i4/002

Shackleton, N. J. (1985). Oceanic carbon isotope constraints on oxygen and carbon dioxide in the Cenozoic atmosphere. *Carbon Cycle Atmospheric CO_2: Natural Variations Archean Present* 32, 412–417.

Sinton, C. W., and Duncan, R. A. (1998). 40Ar-39Ar ages of lavas from the southeast Greenland margin, ODP leg 152 and the rockall plateau, DSDP leg 81. *Proc. Ocean Drill. Program Sci. Results* 152, 387–402.

Speijer, R. P. (2003). "Danian–Selandian sea-level change and biotic excursion on the southern Tethyan margin (Egypt)," in *Causes and consequences of globally warm climates in the early Paleogene*. Editors S. L. Wing, P. D. Gingerich, B. Schmitz, and E. Thomas (Geological Society of America Special Paper), 275–290.

Sprong, J., Kouwenhoven, T. J., Bornemann, A., Dupuis, C., Speijer, R. P., Stassen, P., et al. (2013). In search of the latest danian event in a paleobathymetric transect off kasserine island, north-central Tunisia. *Palaeogeogr. Palaeoclimatol. Palaeoecol.* 379–380, 1–16. doi:10.1016/j.palaeo.2013.01.018

Sprong, J., Kouwenhoven, T. J., Bornemann, A., Schulte, P., Stassen, P., Steurbaut, E., et al. (2012). Characterization of the Latest Danian Event by means of benthic foraminiferal assemblages along a depth transect at the southern Tethyan margin (Nile Basin, Egypt). *Mar. Micropaleontol.* 86–87, 15–31. doi:10.1016/j.marmicro.2012.01.001

Sprong, J., Youssef, M., Bornemann, A., Schulte, P., Steurbaut, E., Stassen, P., et al. (2011). A multi-proxy record of the latest danian event at gebel Qreiya, Eastern Desert, Egypt. *J. Micropalaeontol.* 30, 167–182. doi:10.1144/0262-821x10-023

Van Eijden, A. J. M. (1995). Morphology and relative frequency of planktic foraminiferal species in relation to oxygen isotopically inferred depth habitats. *Palaeogeogr. Palaeoclimatol. Palaeoecol.* 113, 267–301. doi:10.1016/0031-0182(95)00057-s

Wade, B. S., Pearson, P. N., Berggren, W. A., and Pälike, H. (2011). Review and revision of Cenozoic tropical planktonic foraminiferal biostratigraphy and calibration to the geomagnetic polarity and astronomical time scale. *Earth Sci. Rev.* 104, 111–142. doi:10.1016/j.earscirev.2010.09.003

Westerhold, T., Röhl, U., Donner, B., McCarren, H. K., and Zachos, J. C. (2011). A complete high-resolution Paleocene benthic stable isotope record for the central Pacific (ODP Site 1209). *Paleoceanography* 26, PA2216. doi:10.1029/2010PA002092

Westerhold, T., Röhl, U., Raffi, I., Fornaciari, E., Monechi, S., Reale, V., et al. (2008). Astronomical calibration of the Paleocene time. *Palaeogeogr. Palaeoclimatol. Palaeoecol.* 257 (4), 377–403. doi:10.1016/j.palaeo.2007.09.016

Youssef, A. M. (2009). High resolution calcareous nannofossil biostratigraphy and paleoecology across the Latest Danian event (LDE) in central Eastern Desert, Egypt. *Mar. Micropaleontol.* 72, 111–128. doi:10.1016/j.marmicro.2009.03.007